

40SiO₂-40P₂O₅-20ZrO₂ sol-gel infiltrated sSEBS membranes with improved methanol crossover and cell performance for direct methanol fuel cell applications

 The corrections made in this section will be reviewed and approved by a journal production editor.

Ó. Santiago^{a,b,*} oscar.santiago.carretero@upm.es, J. Mosa^c, P.G. Escribano^d, E. Navarro^b, E. Chinarro^c, M. Aparicio^c, T.J. Leo^a, C. del Río^d

^aDept. Arquitectura, Construcción y Sistemas Oceánicos y Navales, ETSI Navales, Universidad Politécnica de Madrid, Avda. de La Memoria 4, Madrid 28040, Spain

^bDept. Mecánica de Fluidos y Propulsión Aeroespacial, ETS Ingeniería Aeronáutica y Del Espacio, Universidad Politécnica de Madrid, Plz. Cardenal Cisneros 3, Madrid 28040, Spain

^cInstituto de Cerámica y Vidrio (ICV-CSIC), Kelsen 5, 28049 Madrid, Spain

^dInstituto de Ciencia y Tecnología de Polímeros (ICTP-CSIC), Juan de La Cierva 3, 28006 Madrid, Spain

* *Corresponding author.* Dept. Arquitectura, Construcción y Sistemas Oceánicos y Navales, ETSI Navales, Universidad Politécnica de Madrid, Avda. de la Memoria 4, Madrid 28040, Spain.

Abstract

Membranes commonly used in direct methanol fuel cell (DMFC) are expensive and show a great permeability to methanol which reduces fuel utilization and leads to mixed potential at the cathode. In this work, sulfonated styrene-ethylene-butylene-styrene (sSEBS) modified membranes with zirconia silica phosphate sol-gel phase are developed and studied in order to evaluate their potential use in DMFC applications. The synthesized hybrid membranes and sSEBS are subjected to an exhaustive physicochemical characterization by liquid uptake, ion exchange capacity, atomic force microscopy, X-ray photoelectron spectroscopy and dynamic mechanical and thermogravimetric analyses. Likewise, the potential use of the prepared membranes in DMFC is evaluated by means of electrochemical characterizations in single cell, determining the limiting methanol crossover current densities, proton conductivities and DMFC performances. The hybrid membranes show lower water and methanol uptakes, higher stiffness, water retention capability, upper power density and lower methanol crossover than sSEBS and Nafion 112.

Keywords: Proton exchange membrane; Crossover; Direct methanol fuel cell; Phosphosilicate; Sol-gel hybrid[Instruction: Is it possible that the Abstract and Keywords keep completely in the first page of the PDF document? In the first page between lines 53 and 59 there is a lot of space.]

Introduction

The global warming derived from greenhouse gas emissions and environmental pollution is a pressing problem for humankind [1]. In this context, the research of new environmentally friendly power sources has been intensified in last decades. Fuel cells, devices that directly convert chemical energy stored in the reactants into electrical energy, arise as a promising technology. In particular, direct methanol fuel cells (DMFCs) are one of the most explored types of fuel cells. As fuel, methanol has a high energy density and since it is liquid at room temperature and atmospheric pressure, it has an easy handling and is safe for distribution and storage [2–4]. These characteristics along with the low DMFC working temperature make DMFCs a suitable technology to power different portable electronics, light-duty traction vehicles and backup systems [5–11]. In fact, they have been successfully operated in systems as demanding as unmanned aerial vehicles [12,13].

However, the use of DMFCs is not yet commercially widespread due to some technical limitations, the main one being the methanol crossover from the anode to the cathode through the membrane [14]. This phenomenon leads to a reduction of the cathode potential and the waste of methanol [15–18]. Typically, Nafion, with suitable chemical and thermal resistances and high proton conductivity, has been the most used compound for DMFC membranes [19,20]. Notwithstanding these good properties, Nafion also shows a high cost and notably methanol permeability, thereby preventing its use in DMFCs [21]. A well-known option to overcome the Nafion problems in DMFC is the synthesis of new economic polymeric membranes with adequate proton conductivities and better methanol crossover resistances being as in DMFC a minor reduction in conductivity is usually accepted in order to reduce the methanol permeability and thus improve the fuel conversion efficiency [22–25].

In this regard, styrene-ethylene-butylene-styrene triblock copolymer (SEBS) is an interesting and low cost raw material for fuel cell applications as it becomes a proton conducting ionomer by direct sulfonation reaction of styrenic units [26–29]. Nevertheless, although low cost electrolyte sSEBS membranes with high proton conductivity can be easily synthesized they experience an unacceptable loss of dimensional stability and mechanical weakness in wet state that seriously compromises their lifetime and durability. That is why DMFC performance of membrane electrodes assemblies (MEAs) based on sSEBS as proton exchange membrane (PEM) are rarely reported in spite of its cost effectiveness and lower methanol crossover than perfluorosulfonic acid membranes [30–32].

An interesting attempt to prevent these mechanical limitations as well as controlling methanol crossover in DMFC is the preparation of hybrid PEMs by combining sSEBS with nano-scale inorganic components [30–40]. In this sense, different designs for preparing nanocomposite membranes are available which can be broadly classified into two groups: those based on the addition and mixing of a hydrophilic inorganic solid to a polymer solution (followed by solvent casting) and those based on sol-gel chemistry in which the specific

interactions between components are favored and a more extended inorganic network is generally achieved [41–48].

Among the different approaches developed for the preparation of hybrid membranes, sol-gel chemistry by direct infiltration of an inorganic precursor into sSEBS membranes is an interesting strategy to modify a ionomeric membrane with control of the location of the inorganic network. Taking advantage of the fact that sSEBS is characterized by a well-known morphology with separated microphases where the blocks (ionic and non-ionic) of the copolymer are self-organized into hydrophilic and hydrophobic domains [49–54], the sol-gel infiltration method makes use of such existing hydrophilic regions in a preformed sSEBS membrane as preferential sites (templates) to accommodate the inorganic component only inside of them where hydrolysis and condensation reactions will occur in situ catalyzed by acid media. Thus, the resultant interpenetrating proton-conducting membranes often lead to an improvement in mechanical strength and reactant barrier properties as it was already reported by other authors [31,36].

Pure inorganic electrolytes such as $\text{SiO}_2\text{-P}_2\text{O}_5\text{-ZrO}_2$ have also been synthesized via sol-gel chemistry as proton exchange membranes but their main limitation is a very low mechanical stability [55]. Despite this, these materials may have interesting technological applications not only because of their nanosized porosity, which allows a high retention of water molecules inside the porous texture, but also due to the presence of M – OH surface groups, mainly P–OH, that can assist proton mobility, providing hopping sites for proton conduction [55–59].

In a previous work [60], economic hybrid membranes (organic-inorganic) were developed by sol-gel chemistry and direct infiltration of a novel zirconia modified phosphosilicate gel ($40\text{SiO}_2\text{-}40\text{P}_2\text{O}_5\text{-}20\text{ZrO}_2$) within the sulfonated polystyrene blocks of sSEBS for their use in hydrogen fuel cells (PEMFC). The results showed that infiltration times up to 40 min led to hybrid membranes with lower uptake in water, enhanced dimensional stability, good proton conductivity and better cell performance than pure sSEBS, while a more extended infiltration times (60 min and beyond) led to a sol-gel coating deposited on the membrane surface which was detrimental on all of these membrane properties (chemical stability, proton conductivity and H_2/O_2 cell performance). These are interesting findings, however, the working conditions of membranes in DMFCs and hydrogen PEMFCs are notably different. Unlike hydrogen PEMFCs in which membranes are in continuous contact with humidified gaseous hydrogen, membranes in DMFCs are in contact with an aqueous methanol solution, making dimensional stability and water uptake critical factors. In addition, membranes for DMFCs show the crossover phenomenon which has a great impact in their performances, whereas this phenomenon is negligible in the case of hydrogen fuel cells. Therefore, the aim of this work is to investigate this hybrid membrane preparation anew in order to reduce the methanol crossover with respect to pristine sSEBS and Nafion, thereby improving DMFC performance. In this case, infiltration times up to 40 min are implemented according the results previously reported [60]. A complete physicochemical characterization of the membranes is carried out to explain their behavior in DMFCs. The extent of zirconia modified phosphosilicate infiltration and the location where it takes place are evaluated in terms of liquid uptake (water and methanol), dimensional changes, ion exchange capacity (IEC), morphology (AFM), microstructure (XPS, DMA) and thermal stability (TGA). Membrane-electrodes assemblies (MEAs) are electrochemically characterized in order to determine

methanol crossover, proton conductivity (EIS) and DMFC performance of the new hybrid infiltrated membranes and compare their characteristics with those of Nafion 112 and sSEBS.

Experimental

Materials

Styrene-ethylene-butylene-styrene triblock copolymer (SEBS, Calprene H6120) with 32 wt % of aromatic units and having linear structure was provided by Repsol (Dynasol Group). Inorganic sols were prepared with trimethyl phosphate [$\text{PO}(\text{OCH}_3)_3$, TMP] and zirconium tetrapropoxide [$\text{Zr}(\text{OC}_3\text{H}_7)_4$, TPZr] from Aldrich, tetraethylorthosilicate [$\text{Si}(\text{OC}_2\text{H}_5)_4$, TEOS] from Merck, acetylacetone ($\text{C}_5\text{H}_8\text{O}_2$, acac) from Fluka and hydrochloric acid (catalyst) and propanol (solvent) from Aldrich. Trimethylsilyl chlorosulfonate (Sigma-Aldrich) was used as sulfonation reagent; chloroform (CHCl_3 , Scharlau) and 1,2-dichloroethane (DCE, Scharlau) were used as solvents; sulfuric acid (H_2SO_4 , Aldrich) and methanol (CH_3OH , Honeywell) were utilized to swell the membranes and for electrochemical characterization; potassium hydrogen phthalate (Sigma-Aldrich), sodium chloride (NaCl, Panreac) and sodium hydroxide (NaOH, Panreac) were employed for titration experiments. Millipore water was used to prepare the solutions. All chemicals involved were used as received.

Preparation of $40\text{SiO}_2\text{-}40\text{P}_2\text{O}_5\text{-}20\text{ZrO}_2$ sol-gel solution

TMP, TEOS, propanol (half volume) with a molar ratio propanol/TEOS + TMP + TPZr of 2, and water as HCl 0.1 N (molar ratio of water/TEOS = 1) were mixed by stirring for 2 h. On the other hand, TPZr, propanol (half volume) and acetylacetone (molar ratio of acetylacetone/TPZr = 1) were mixed by stirring for 2 h. Both solutions were mixed and homogenised by stirring for 1 h.

Manufacture of sSEBS membranes and infiltration process

SEBS was dissolved in CHCl_3 (12% wt/vol) in order to obtain thin polymer membranes by doctor blade (BYK Instruments). The sulfonation reaction of styrene units was carried out by immersing the SEBS membranes in trimethylsilyl chlorosulfonate (0.3 M in DCE) during 2 h. Before infiltration, the sulfonated SEBS membranes (sSEBS) were swelled in H_2SO_4 1 N (80 °C, 2 h) and subsequently introduced into the $40\text{SiO}_2\text{-}40\text{P}_2\text{O}_5\text{-}20\text{ZrO}_2$ solution at 80 °C for 5, 20 and 40 min to carry out the infiltration procedure. After that, they were repeatedly washed with ethanol, dried at 50 °C for 1 h and heat treated at 120 °C during 2 h to ensure the consolidation of the inorganic component. To complete the infiltration process, they were again washed with ethanol at 80 °C for 2 h and finally dried at 80 °C for 1 h.

Physico-chemical characterization of hybrid membranes

Liquid uptake and dimensional changes

For uptake degree measurement, membranes of similar sizes were immersed either in deionized water or in 1 M CH_3OH at room temperature for five days when the swelling is considered to be completed. After wiping out excess water at the surface, the wet membranes were quickly weighed (w_{wet}); then, they were dried at

50 °C for 24 h and weighed again (w_{dry}). Thus, the uptake percentage of the films in water and methanol was determined by gravimetric method using Equation (1):

$$\% \text{ uptake} = \frac{w_{wet} - w_{dry}}{w_{dry}} \cdot 100 \quad (1)$$

The dimensional variations (area increase, AI) were calculated under the same conditions of liquid uptake, quantifying the difference of membrane surface area by the following equation:

$$\% \text{ AI} = \frac{A_{wet} - A_{dry}}{A_{dry}} \cdot 100 \quad (2)$$

where, A_{wet} and A_{dry} are the surface area of hydrated and dried membranes, respectively.

Ion exchange capacity (IEC)

The ion-exchange capacity IEC ($\text{meqH}^+\text{g}^{-1}$) was calculated by an acid-base titration. Membranes with known dry mass were equilibrated in 100 mL 1 M NaCl solution for 15 days to replace the H^+ by Na^+ ions. The released protons in solution were titrated with 0.01 M NaOH to a phenolphthalein endpoint. The IEC was obtained by the equation:

$$\text{IEC} = \frac{M_{\text{NaOH}} \cdot V_{\text{NaOH}}}{w_{dry}} \quad (3)$$

where M_{NaOH} is the molar concentration of the titrant, V_{NaOH} is the added titrant volume at the equilibrant point and w_{dry} is the dried weight of the sample. Each titration was performed in triplicate and the average value was taken as final IEC.

Atomic force microscopy (AFM)

Atomic Force Microscopy measurements were performed in dry state membranes using a Cervantes AFM System (Nanotec Electronica S.L., SPAIN).

X-ray photoelectron spectroscopy (XPS)

Spectra were performed on a K-Alpha – Thermo Scientific spectrometer with monochromatic Al $\text{K}\alpha$ X-ray source (1486.68 eV). Compositional depth profiles of the hybrid membranes were obtained to evaluate the homogeneity of elements distribution through the thickness. Surface chemical states of hybrid membranes with different oxidation states were also evaluated by XPS using an Ar^+ ion source. Elements quantification was

achieved using the Shirley method for complete spectra and a peak-fit program (Advantage 4.6 Thermo) for oxygen, zirconium, silicon, sulfur and phosphorus spectra.

Dynamic mechanical analysis (DMA)

Dynamic mechanical properties were evaluated using a TA Instrument 983 dynamic mechanical analyzer in tension mode. The samples were thermal treated from -100 to 260 °C, at 10 Hz with a heating rate of 2 °C min^{-1} . The geometry used was the stress pattern. The strength applied was 0.5 N, and the shifts varying between 8 and 40 μm .

Thermogravimetric analysis (TGA)

Thermal stability (10 – 15 mg) was analyzed by TGA using a TA Instruments TA-Q500 equipment. The samples were treated to 800 °C at 10 °C min^{-1} in air, and the degradation temperature, weight loss and remaining residue at 800 °C were measured.

Electrochemical characterization of membrane-electrodes assembly (MEA's)

MEA's fabrication

To evaluate the potential application in fuel cells, MEAs with pure polymeric and hybrid membranes were tested in a single DMFC (3.8 cm^2 of active area). The electrodes were made following the procedure described by Jurado et al. [61] which consists in a catalytic layer airbrushed onto a gas diffusion layer (GDL, non-woven carbon paper gas diffusion media with a Microporous Layer (MPL) and PTFE treated to 5% (SIGRACET 39BC GDL)). The ink to prepare the catalytic layer of both electrodes consisted in a suspension in a ratio of 7:3 of the electrocatalyst and solution of ionomer (Aldrich 5 wt% Nafion® solution) and a mixture of H_2O : isopropanol (2:1). Anode was prepared with 40% PtRu (1:1) on carbon Vulcan XC72 (E-TEK) as electrocatalyst, with a PtRu load of 3 mg cm^{-2} ; and cathode was fabricated with 40% Pt on carbon Vulcan XC72 (E-TEK) as electrocatalyst and 1 mg cm^{-2} of Pt load.

To prepare the MEAs, each membrane was sandwiched between the electrodes and the set was hot-pressed at 10 bar and 100 °C for about 3 min. Cell hardware consisted of two stainless steel 316L plates with a flow pattern of parallel channels. The whole assembly was clamped by 4 screws with a torque of 2 N m. The described single DMFC was used for methanol crossover determination, through-plane proton conductivity measurements and cell performance. A MEA with Nafion 112 (DuPont) commercial membrane was also prepared and tested as reference material.

Limiting crossover current density

The methodology developed by Ren et al. [62] was followed to measure the limiting crossover current density ($J_{\text{lim,cross}}$). Methanol solution 1 M was supplied to the anode (PtRu/C) at 3 mL min^{-1} and pure nitrogen humidified at 68 °C was supplied to the cathode (Pt/C) at 100 mL min^{-1} . In this case, methanol crossing the assembly is oxidized at the Pt/C electrode by establishing a potential difference. Autolab PGSTAT 128 N in potentiostatic mode was used to measure the current response to the applied potential, which ranged between

0.3 and 0.95 V with 50 mV increments applied over 3 min. Pt/C electrode was used as working electrode and PtRu/C as both counter and reference electrodes. The limiting current density of each current-voltage curve is a measure of methanol flux through the corresponding assembly.

In situ through-plane proton conductivity

The proton conductivity through the plane of the membranes was evaluated by means of electrochemical impedance spectroscopy tests which were performed using a potentiostat/galvanostat, Autolab PGSTAT 128N, coupled to a frequency response analyzer module, FRA 32M. The assembly, reactants and flow rates used were the same as in the previous section. The frequency of the sinusoidal excitation signal ranged from 1 Hz to 100 kHz. The measures were performed at a constant bias potential of 0.3 V with an amplitude of 10 mV. The proton conductivity through the membranes (σ_{TP}) was calculated as follows:

$$\sigma_{TP} = \frac{L}{S \cdot R_{\Omega}} \quad (4)$$

where L represents the membrane thickness, S is the active area and R_{Ω} depicts the resistance obtained from the intersection point of the impedance curve at high frequency and the real impedance axis in the Nyquist plot.

DMFC polarization curve

Polarization curve measures were conducted at 60 °C supplying 1 M methanol solution at 3 mL min⁻¹ and pure humidified oxygen at 100 mL min⁻¹ and 1 bar to anode and cathode, respectively. A warm-up phase, consisting of thermal and electrical conditioning, was carried out before recording polarization curves. Firstly, with the aid of a heat exchanger, the cell was heated up to the operating temperature (60 °C). Then, two potential step cycles from the open circuit voltage to 0.4 V were conducted to activate the catalysts, each step is applied over 180 s. The experimental setup used to perform the polarization curve measures was a homemade test bench, which has been previously described [63].

Results and discussion

Hybrid membrane characterization

Liquid uptake and dimensional changes

Since water serves as the conducting medium of protons, water uptake is a critical factor that noticeably affects the proton conductivity of sulfonated polymers. Thus, in this sense, achieving an optimal level of hydration is absolutely necessary. However, if the uptake degree reaches an excessive value the dimensional stability and mechanical integrity of the membrane can be seriously compromised. According the data shown in Table 1, the infiltration of the sol-gel solution within the hydrophilic blocks of sSEBS reduces the undesirable uptake in liquid (water or methanol), decreasing the dimensional changes of the sulfonated polymer. Consequently, the

infiltrated membranes take up a smaller amount of liquid than the pure polymer as infiltration time increases. The same behavior is perceived regarding the area increase. On the other hand, the membranes weight after infiltration shows a continuous increment which is indicative that the infiltration procedure gives rise to the formation of an increasingly wide inorganic-organic network. Likewise, as the infiltration time increases, the area of the membrane decreases. The embedding of the zirconia modified phosphosilicate gel network into ionic domains is able to modify the microstructure of liquid filled channels, decreasing uptake and hence enhancing the mechanical integrity of the membrane. Similar enhancements in reducing methanol permeability are expected to take place for the more infiltrated hybrids.

alt-text: Table 1

Table 1

i The table layout displayed in this section is not how it will appear in the final version. The representation below is solely purposed for providing corrections to the table. To preview the actual presentation of the table, please view the Proof.

Dimensional changes, uptake degree and ion exchange capacity for sSEBS and hybrid membranes. (Some of these data have been extracted from Ref. [60]).

Membrane	Weight Increase (%)	Area Increase (%)	Water uptake (%)	Methanol uptake (%)	IEC (meqH ⁺ g ⁻¹)
sSEBS	–	–	203.3	209.3	1.77
5 min	3.2	116.9	156.5	148.1	1.62
20 min	4.0	93.6	105.2	110.3	1.28
40 min	7.1	88.7	89.2	96.7	1.23

Ion exchange capacity (IEC)

Table 1 compiles the IEC (meqH⁺ g⁻¹) values of pure polymer and infiltrated membranes. According to the tendency of liquid uptake discussed above, the IEC values for hybrid membranes are always lower than for pure polymer and decrease as infiltration time progresses which are indicating that the inorganic precursor diffuses and grows into the ionic blocks of the copolymer where the sol-gel reactions come about.

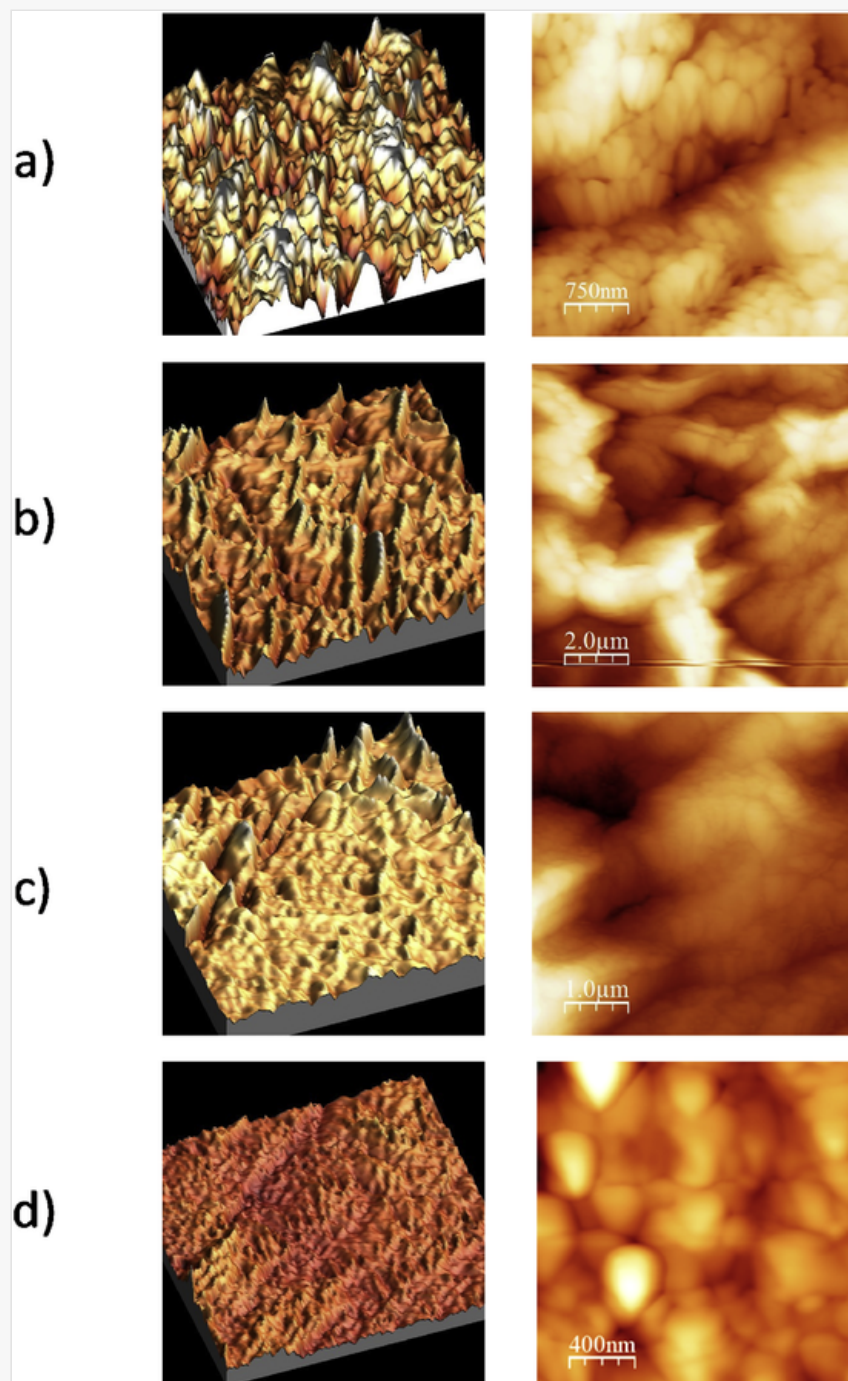
Atomic force microscopy (AFM)

AFM images of pure and infiltrated sSEBS membranes in dry state are presented in Fig. 1. The topography of pure sSEBS shows the typical microphase separation of sSEBS with dark areas corresponding to hydrophilic blocks related to sulfonate groups containing interconnected nano-channels of about 10 nm average width. Furthermore, the light regions correspond to hydrophobic domains constituted by the polymer backbone that look like lamellar structures of 30–40 nm. All infiltrated membranes show the typical sSEBS microstructure

with well-ordered and continuous ionic channels formed by the microphase separation between hydrophilic domains and hydrophobic domains [64]. Based on these results, the infiltration during 40 min produces a flatter topography due to a deeper procedure, as it is shown in the three dimensional image (Fig. 1d left). Also, the channels width of the hydrophilic regions (dark areas) is reduced with the infiltration time, suggesting that the inorganic component is filling primarily the hydrophilic domains of the polymer matrix, limiting the methanol molecules diffusion [65].

alt-text: Fig. 1

Fig. 1



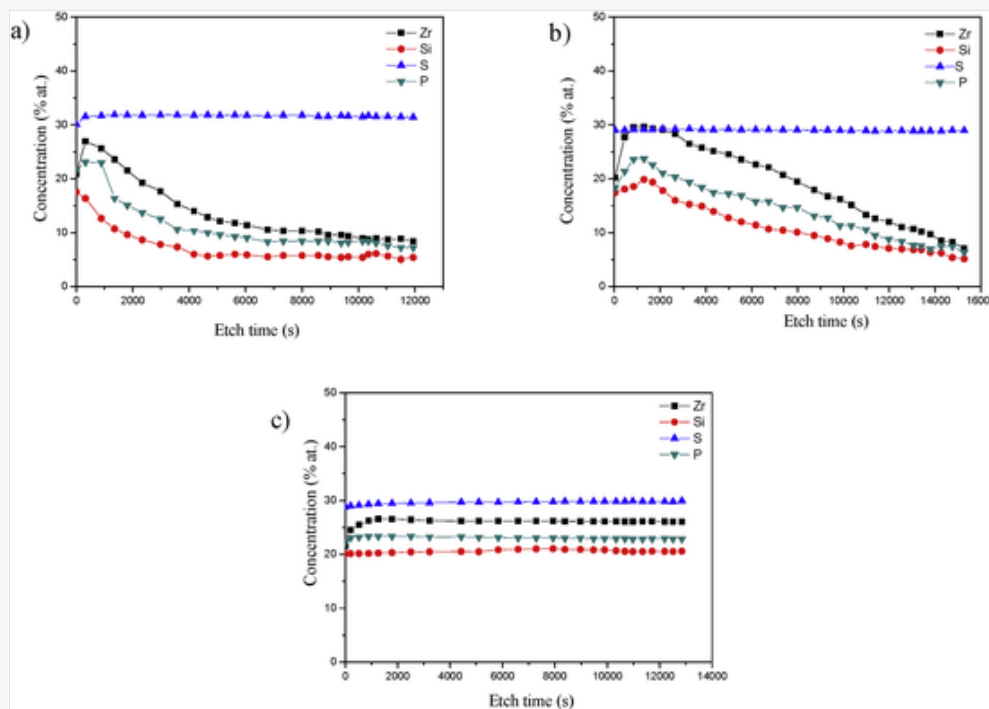
Three-dimensional (left) and surface (right) AFM images of a) sSEBS and hybrid membranes at different infiltration times b) 5 min, c) 20 min and d) 40 min.

X-ray photoelectron spectroscopy (XPS)

The XPS depth profiles of the sSEBS hybrid membranes can be observed in Fig. 2 at different immersion times. Sulfur profile keeps almost constant for all infiltration times meaning that sulfonation was performed successfully. Zirconium, silicon and phosphorus profiles change with the infiltration time reaching to a uniform profile at 40 min. This result is in agreement with EDX results previously reported [60]. It seems that infiltration is more efficient along the edge of the membrane at 5 and 20 min of immersion times, and it takes longer time to incorporate the inorganic phase into the interior areas. Zirconium and phosphorus lines present higher energy than silicon. Surface chemical XPS analysis does not detected differences in oxidation states of the different elements P, Zr, Si and S indicating that ionic conductivity is not expected.

alt-text: Fig. 2

Fig. 2



XPS depth profiles of hybrid membranes at different infiltration times: a) 5 min, b) 20 min and c) 40 min.

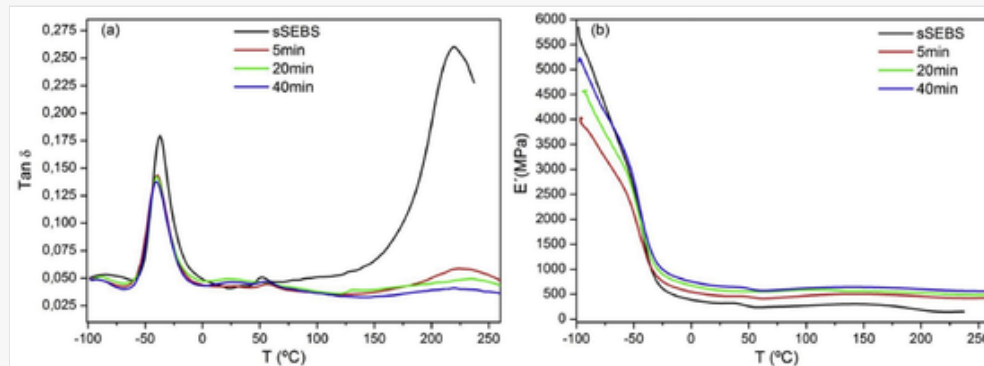
Dynamic mechanical analysis (DMA)

DMA is used to analyze the viscoelastic behavior of the membranes in terms of loss factor ($\tan \delta$) and storage modulus (E') as well as the influence of the inorganic additive on their mechanical strength. The final objective pursued with the incorporation of the inorganic component into the polymer matrix is to achieve longer lifetime membranes with better DMFC performance than pure sSEBS which is related undoubtedly to

getting improvement of the mechanical properties. The $\tan \delta$ curves versus temperature of sSEBS and infiltrated membranes for 5, 20 and 40 min are shown in Fig. 3a.

alt-text: Fig. 3

Fig. 3



DMA analysis of sSEBS and hybrid membranes. (a) loss factor ($\tan \delta$) vs temperature and (b) storage modulus (E') vs temperature.

Two distinctive glass transition temperatures are detected; one at low temperature corresponds to the ethylene-butylene blocks (T_g^{EB}) and the other is associated to the sulfonated polystyrene blocks (T_g^{PS}) and observed at higher temperature. Fig. 3a shows that the presence of the inorganic component has minor influence on the first relaxation given that the peak temperature and shape appear essentially equal to that for pure sSEBS. On the contrary, T_g^{PS} is markedly influenced not only in a variation to higher temperature which is due to strong hydrogen bond interactions between sulfonic acid groups in PS blocks and hydrolyzed inorganic zirconia modified phosphosilicate but primarily in the values of $\tan \delta$, suggesting that infiltration process has been efficient so phosphosilicate gel lives within ionic domains mainly. The severe reduction in $\tan \delta$ values for hybrids is likely related to the higher stiffness of these materials due to the restriction on the chain mobility in the ionic domains imposed by the inorganic network respect to the pure sulfonated polymer. Thus, Fig. 3b represents the storage modulus (E') versus temperature where E' values increase in all hybrid membranes in comparison to sSEBS along the rubbery plateau and over infiltration time. For example, at 60 °C the values of E' are 237 MPa for sSEBS and 413 MPa, 551 MPa and 570 MPa for the respective hybrids as infiltration time is progressing. It is reasonable that zirconia modified phosphosilicate gel lead to the formation of stronger hydrogen bond interactions besides the already existing between sulfonic acid groups, increasing rigidity in the hybrid membranes.

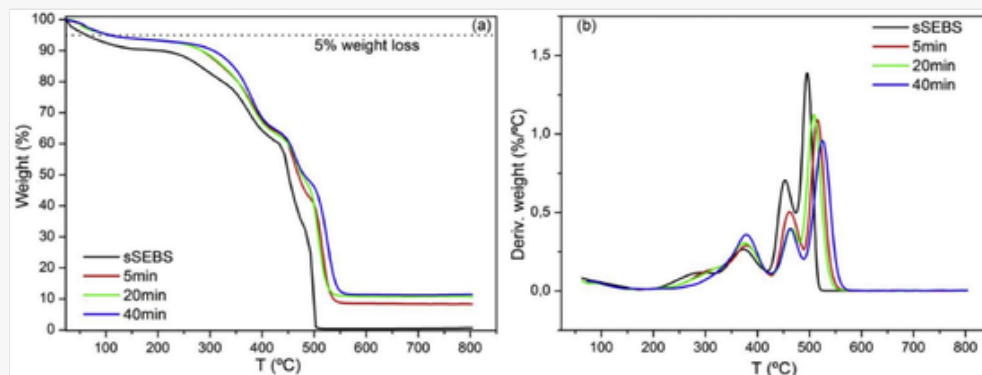
Thermogravimetric analysis (TGA)

The degradation temperatures, weight losses and inorganic remaining residues at 800 °C were evaluated by means of TGA. Three consecutive stages of degradation are usually observed in this type of sulfonated polymers: loss of absorbed water and residual organic solvents (<200 °C); decomposition of sulfonic acid groups ($-SO_3H$) (270–400 °C) and oxidative degradation of main polymer chain above 400 °C. The TGA

curves of weight loss and derivative weight loss versus temperature of sulfonated polymer and hybrid membranes are shown in Fig. 4a and b, respectively.

alt-text: Fig. 4

Fig. 4



TGA analysis of sSEBS and hybrid membranes. (a) weight loss vs temperature and (b) derivative weight loss vs temperature.

The results indicate that all hybrid membranes retain more water than pure polymer since the weight losses connected to the first stage of dehydration are much lower than in sSEBS. Thus, a weight loss of 5% occurs at 63 °C for sSEBS; at 103 °C for 5 and 20 min samples and at 113 °C for the membrane infiltrated for the longest time, 40 min. This fact is very interesting since besides taking less water than sSEBS (lower water uptake), these hybrid membranes are able to preserve it at higher temperatures. The interaction established between the hydrolyzed inorganic zirconia modified phosphosilicate surface groups (Si-OH and P-OH), the sulfonic acid groups of sSEBS and the water molecules can help to explain this behavior as water results in tighter bound to the ionic phase after infiltration. The same pattern is observed in desulfonation and polymer degradation processes because both extend to a broader range of temperature for hybrid membranes in comparison to sSEBS (Fig. 4b). The in-situ sol-gel reaction makes the composite membranes more thermally stable than the pure sulfonated copolymer. This enhancement of the thermal stability after inorganic incorporation is due to the restriction imposed by the presence of the zirconia modified phosphosilicate network and its interaction with sulfonic acid groups. At 800 °C, the interval of the remaining residues ranges between 8.4 and 11.5 wt % according increasingly longer infiltration times.

Electrochemical characterization of the MEA's

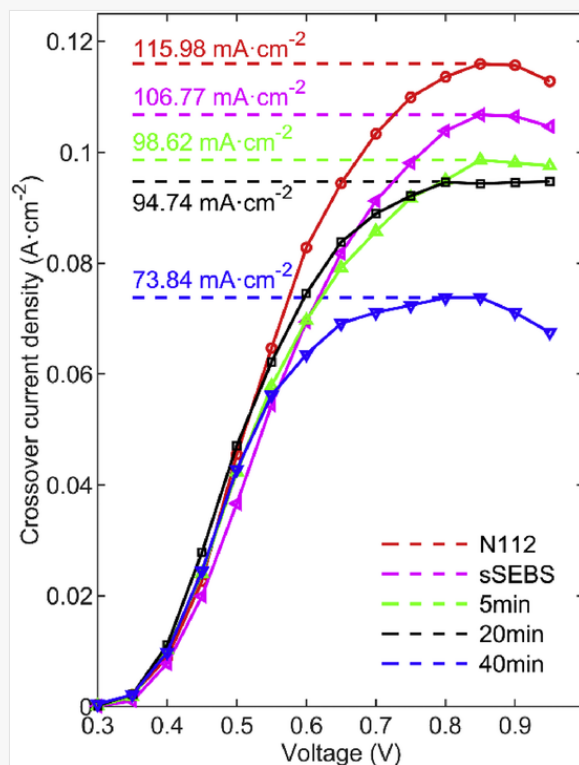
This section aims to compare the behavior of the different membranes, included Nafion 112, in DMFCs. In this regard, all measurements were carried out under the same experimental conditions and with the same single cell and electrodes (new for each MEA) in such a way that the variations in limiting crossover current density, proton conductivity and performance are only due to the membrane used in each case.

Limiting methanol crossover current density and proton conductivity

The current density produced by the oxidation of methanol that crosses the assembly versus the applied potential is shown in Fig. 5, the maximum current density of each MEA represents their limiting crossover current density ($j_{lim,cross}$). The methanol crossover through the membrane is a key factor in DMFC operation that should be reduced in order to maximize the fuel utilization and the potential at the cathode [66]. In this respect, and as can be seen in Fig. 5, the starting polymeric material shows better methanol barrier properties than Nafion 112, as evidenced by its slightly lower limiting methanol current density. In addition, the methanol permeability in the hybrid membranes decreases over infiltration time. Consequently, the membrane infiltrated for the longest time, 40 min, exhibits the lowest $j_{lim,cross}$ value (73.8 mA cm^{-2}) which is notably lower than that of sSEBS and Nafion 112, 107.0 mA cm^{-2} and 115.9 mA cm^{-2} , respectively. The limiting crossover current densities measured are representative of the DMFC methanol crossover at the open circuit voltage but somewhat lower [67].

alt-text: Fig. 5

Fig. 5



Limiting current densities of methanol crossover of the DMFC for MEAs with different membranes.

The results obtained are in good agreement with the water-methanol uptake tests, the topography of hybrid membranes determined by AFM and the XPS depth profiles of the samples. In fact, the closely limiting crossover current density values of the samples infiltrated for 5 and 20 min are consistent with their similar XPS profiles. Likewise, the homogeneous profile of infiltrated species across the membrane infiltrated for 40 min is identified with its lowest limiting crossover current density detected. This reduction as infiltration

time is longer implemented is probably due to the barrier effect exerted by the growing of the zirconia modified phosphosilicate gel network within the hydrophilic domains [68].

The in-situ proton conductivities of the membranes have been calculated from the corresponding Nyquist diagrams of the MEAs obtained by means of EIS (plots not shown). The impedance analysis of the different MEAs have been carried out under the same experimental conditions (1 M CH₃OH anode at 3 mL min⁻¹ and 100 mL min⁻¹ N₂ hydrated at 68 °C cathode, 60 °C cell temperature, torque of 2 N m) in order to compare the results. Under these conditions, MEAs with sSEBS and infiltrated membranes show similar proton conductivity values, $(2.0 \pm 0.5) \cdot 10^{-2}$ S cm⁻¹, which indicate on the one hand, that the percolation within the ionic channels is preserved over infiltration even when both the uptake degree and IEC are lower and, on the other hand, that the strong interactions by hydrogen bonding established between P-OH, Si-OH, Zr-OH and SO₃H groups favour a Grotthus-type mechanism for proton conduction [69].

An illustration of a possible hybrid structure can be observed in Fig. 6, showing the characteristic microphase separated morphology of SEBS before infiltration which is self-organized into hydrophilic and hydrophobic domains and also the sulfonic acid groups grafted to the SEBS structure. After infiltration, the structure shows the sol-gel matrix formation onto the hydrophilic domains by in situ polycondensation. The hybrid structure generated allows the movement of protons jumping from water, sulfonic acid and hydroxyl groups as hopping sites to generate fast proton conduction paths. The presence of inorganic component onto hydrophilic areas reduces in an effective way the methanol crossover.

alt-text: Fig. 6

Fig. 6

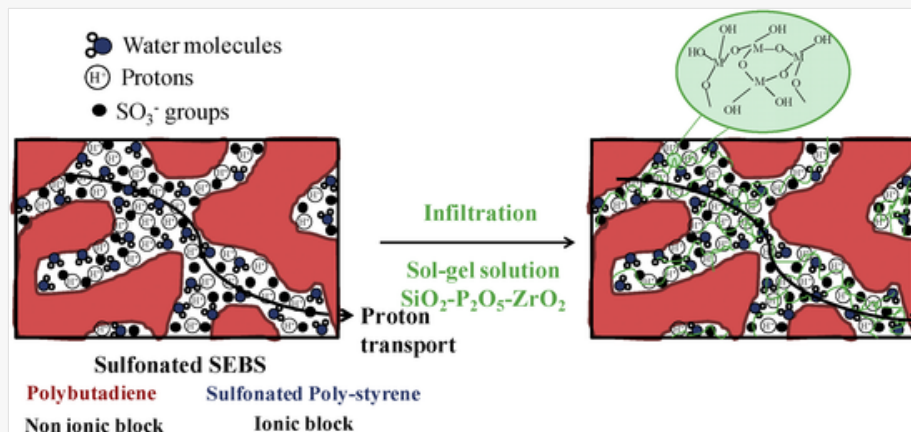


Illustration of the hybrid structure simulating the proton transport through the membrane.

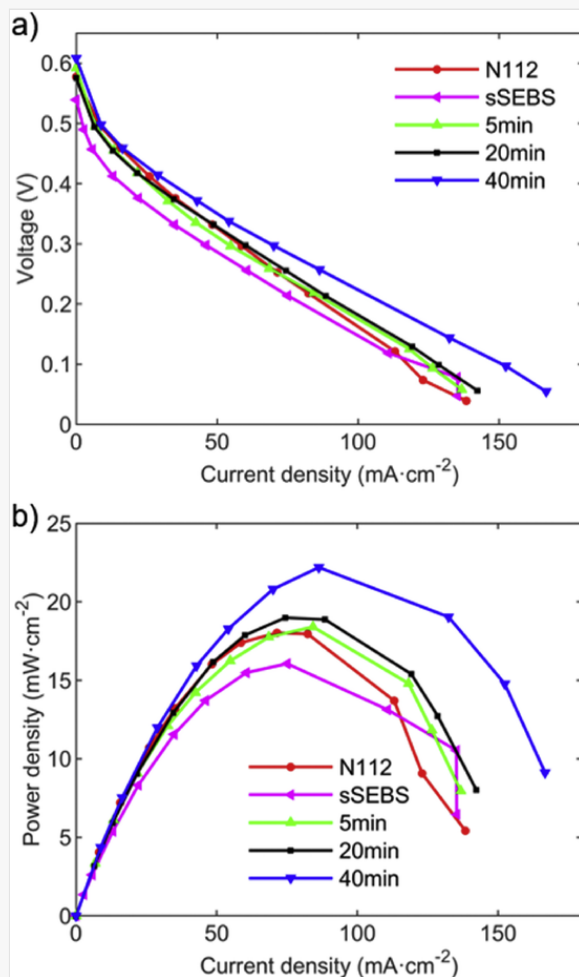
DMFC performance

In order to evaluate the possible use of these hybrid membranes in DMFC, performance tests were carried out in a single direct methanol fuel cell. The cell hardware used had an active area of 3.8 cm² and it was continuously supplied with 1 M CH₃OH and pure humidified oxygen to anode and cathode, respectively.

Fig. 7 represents the polarization and power density curves of pure polymer sSEBS, hybrid membranes with different levels of infiltration, and Nafion 112 as reference material.

alt-text: Fig. 7

Fig. 7



Comparison of DMFC performances for the MEAs with different membranes. a) polarization curves, b) power density curves.

With respect to polarization curves Fig. 7a shows that OCV values of hybrid membranes are higher than that of sSEBS in all cases and they tend to increase over infiltration time. Thus, OCV of sSEBS takes the value of 539 mV while 592 mV, 575 mV and 608 mV are the OCV for 5, 20 and 40 min, respectively, representing increases of 9.8%, 6.7% and 12.8% compared to the OCV of sSEBS. In addition, the average of the OCVs of each membrane (in Fig. 7 only the best polarization curve of each membrane is represented) are 545.6 mV, 568.3 mV, 564.6 mV, 581.9 V and 541.0 mV for sSEBS, 5min, 20min, 40min and Nafion 112, respectively. This behavior may be attributed to the minor methanol crossover of hybrid membranes as the infiltration time increases [70], which is in agreement with the limiting crossover current densities obtained. The lower the methanol crossover is, the lower the mixed potential at the cathode and therefore the higher the OCV. Likewise, the membranes with longer infiltration times showed better performances at low current densities.

In the same way, it can be seen that an increase of infiltration time within the range under study leads to an improvement of the maximum power density (Fig. 7b). Thus, the performance of 40 min membrane stands out above the rest showing the highest maximum power density, 22.2 mW cm^{-2} , and maximum current density, 166.7 mA cm^{-2} . Under the same experimental conditions, sSEBS membrane reaches a maximum power density of 16.1 mW cm^{-2} and a maximum current density of 135.3 mA cm^{-2} , while in the case of Nafion 112 membrane these values are 18.0 mW cm^{-2} and 138.4 mA cm^{-2} , respectively. These results clearly show the best performance in single DMFC of the infiltrated membranes with respect to pure polymer, specially 40 min membrane which shows improvements in both maximum power density and maximum current density of 37.9% and 23.2% with regard to sSEBS membrane. This behavior can be explained on the basis of the extended barrier effect with the infiltration time which leads to lower methanol crossover, appropriate water retention, enough proton conductivity as well as improved mechanical and dimensional stability.

Conclusions

Infiltrated hybrid membranes based on sSEBS and $40\text{SiO}_2\text{-}40\text{P}_2\text{O}_5\text{-}20\text{ZrO}_2$ were prepared by sol-gel method. The initial pursued of reducing uptake degree (water and methanol), dimensional changes and methanol crossover in comparison to pure sSEBS was successfully achieved. Similarly, it was proven by means of XPS that the concentration profiles of infiltrated elements across the membrane thickness were more homogeneous as the infiltration time increases obtaining completely uniform profiles for 40 min infiltrated membrane.

DMA analysis confirmed, on the one hand, that the phase separated morphology of sSEBS was preserved after infiltration process and, on the second hand, that the growth of sol-gel zirconia modified phosphosilicate network took place only into the ionic phase of the copolymer. The strong hydrogen bond interactions between Si-OH, P-OH and $\text{-SO}_3\text{H}$ groups was responsible for the higher stiffness of the hybrid materials compared with sSEBS, as storage modulus (E') values increased over infiltration time. TGA results indicated that infiltrated membranes presented a higher water retention capability than sSEBS in the temperature range corresponding to dehydration. Also, a greater thermal stability was observed as the infiltration time increased. The amount of residue detected confirmed that the level of solid embedded is a function of infiltration time.

The methanol permeability of the hybrid membranes decreases when infiltration time increases, as evidenced by the reduction of the limiting methanol crossover current density, especially for 40 min infiltrated membrane which showed a value 1.45 times lower than sSEBS, in agreement with uptake, XPS and AFM tests. The homogeneous profile of species across the 40 min membrane, in combination with the methanol barrier effect provided by the inorganic filler, led to an important reduction of methanol crossover. Moreover, the infiltrated membranes showed suitable proton conductivity values higher than 0.01 S cm^{-1} . Polarization curve experiments underlined the potential use in DMFCs of the synthesized hybrid membranes. Specially, the membrane infiltrated for 40 min showed an outstanding performance with an OCV 12.8% higher than that of the pure polymer membrane which could be associated with the minor methanol crossover through the membrane. Likewise, this membrane achieved a maximum power density 37.9% greater than that of the sSEBS membrane. Therefore, the outstanding behavior of the synthesized hybrid infiltrated membranes with respect to liquid uptake, dimensional and thermal stabilities, methanol permeability and single DMFC


performance, together with the affordable materials and preparation costs, make them an ideal alternative for use in DMFCs.

Acknowledgements

The authors would like to acknowledge Comunidad de Madrid and European Social Fund (ESF) through the Project S2013/MAE-2975 PILCONAER. The Spanish Ministry of Economy, Industry and Competitiveness is also thanked for the Research Projects MINECO ENE2013-49111-C2-1-R, ENE2014-53734-C2-2-R, ENE2017-86711-C3-1-R, ENE2017-86711-C3-2-R and ENE2017-90932-REDT.

The technical and human support provided by Daniel Gamarra (Facility of Analysis and Characterization of Solids and Surfaces of SAIUEX, financed by UEX, Junta de Extremadura, MICINN, FEDER and FSE) is recognized. The authors wish to thank Dr. Sara Serena, Rosa Navidad, Desiree Ruiz and Esther Blazquez for their support and help in the experimental procedure.

References

 The corrections made in this section will be reviewed and approved by a journal production editor. The newly added/removed references and its citations will be reordered and rearranged by the production team.

- [1] UNFCCC Adoption of the paris agreement. 2015. FCCC/CP/2015/L.9/Rev.1.
- [2] Gong A., Verstraete D. Fuel cell propulsion in small fixed-wing unmanned aerial vehicles: current status and research needs. *Int J Hydrogen Energy* 2017;42:21311–21333.
- [3] Abdul Sathar Eqbal M., Fernando N., Marino M., Wild G. Hybrid propulsion systems for remotely piloted aircraft systems. *Aerospace* 2018;5:34.
- [4] Fadzillah D.M., Kamarudin S.K., Zainoodin M.A., Masdar M.S. Critical challenges in the system development of direct alcohol fuel cells as portable power supplies: an overview. *Int J Hydrogen Energy* 2019;44:3031–3054.
- [5] Barbera O., Stassi A., Sebastian D., Bonde J.L., Giacoppo G., D’Urso C., et al. Simple and functional direct methanol fuel cell stack designs for application in portable and auxiliary power units. *Int J Hydrogen Energy* 2016;41:12320–12329.
- [6] Wang L., He M., Hu Y., Zhang Y., Liu X., Wang G. A “4-cell” modular passive DMFC (direct methanol fuel cell) stack for portable applications. *Energy* 2015;82:229–235.
- [7] Ong B.C., Kamarudin S.K., Basri S. Direct liquid fuel cells: a review. *Int J Hydrogen Energy* 2017;42:10142–10157.
- [8] Müller M., Kimiaie N., Glösen A. Direct methanol fuel cell systems for backup power—influence of the standby procedure on the lifetime. *Int J Hydrogen Energy* 2014;39:21739–21745.

- [9] Wang L., Yuan Z., Wen F., Cheng Y., Zhang Y., Wang G. A bipolar passive DMFC stack for portable applications. *Energy* 2018;144:587–593.
- [10] Masdar M.S., Zainoodin A.M., Rosli M.I., Kamarudin S.K., Daud W.R.W. Performance and stability of single and 6-cell stack passive direct methanol fuel cell (DMFC) for long-term operation. *Int J Hydrogen Energy* 2017;42:9230–9242.
- [11] Baglio V., Stassi A., Barbera O., Giacoppo G., Sebastian D., D’Urso C., et al. Direct methanol fuel cell stack for auxiliary power units applications based on Fumapem® F-1850 membrane. *Int J Hydrogen Energy* 2017;42:26889–26896.
- [12] González-Espasandín Ó., Leo T.J., Navarro-Arévalo E. Fuel cells: a real option for unmanned aerial vehicles propulsion. *Sci World J* 2014;2014:1–12.
- [13] Kang K., Park S., Cho S.O., Choi K., Ju H. Development of lightweight 200-W direct methanol fuel cell system for unmanned aerial vehicle applications and flight demonstration. *Fuel Cell* 2014;14:694–700.
- [14] Shukla A., Dhanasekaran P., Sasikala S., Nagaraju N., Bhat S.D., Pillai V.K. Nanocomposite membrane electrolyte of polyaminobenzene sulfonic acid grafted single walled carbon nanotubes with sulfonated polyether ether ketone for direct methanol fuel cell. *Int J Hydrogen Energy* 2019;44:27564–27574.
- [15] Kumar P., Dutta K., Das S., Kundu P.P. An overview of unsolved deficiencies of direct methanol fuel cell technology: factors and parameters affecting its widespread use. *Int J Energy Res* 2014;38:1367–1390.
- [16] Colpan C.O., Ouellette D., Glüsen A., Müller M., Stolten D. Reduction of methanol crossover in a flowing electrolyte-direct methanol fuel cell. *Int J Hydrogen Energy* 2017;42:21530–21545.
- [17] Heinzl A., Barragan V.M. A review of the state-of-the-art of the methanol crossover in direct methanol fuel cells. *J Power Sources* 1999;84:70–74.
- [18] Mohammed H., Al-Othman A., Nancarrow P., Tawalbeh M., Assad M.E.H. Direct hydrocarbon fuel cells: a promising technology for improving energy efficiency. *Energy* 2019;172:207–219.
- [19] Cheng X., Peng C., You M., Liu L., Zhang Y., Fan Q. Characterization of catalysts and membrane in DMFC lifetime testing. *Electrochim Acta* 2006;51:4620–4625.
- [20] Baglio V., Arico A.S., Di Blasi A., Antonucci V., Antonucci P.L., Licoccia S., et al. Nafion–TiO₂ composite DMFC membranes: physico-chemical properties of the filler versus electrochemical performance. *Electrochim Acta* 2005;50:1241–1246.
- [21] Hosseinpour M., Sahoo M., Perez-Page M., Baylis S.R., Patel F., Holmes S.M. Improving the performance of direct methanol fuel cells by implementing multilayer membranes blended with cellulose nanocrystals. *Int J Hydrogen Energy* 2019;44:30409–30419.

- [22] Kim H., Prakash S., Mustain W.E., Kohl P.A. Sol-gel based sulfonic acid-functionalized silica proton conductive membrane. *J Power Sources* 2009;193:562–569.
- [23] Cho K.Y., Eom J.Y., Jung H.Y., Choi N.S., Lee Y.M., Park J.K., et al. Characteristics of PVdF copolymer/Nafion blend membrane for direct methanol fuel cell (DMFC). *Electrochim Acta* 2004;50:583–588.
- [24] You P.Y., Kamarudin S.K., Masdar M.S. Improved performance of sulfonated polyimide composite membranes with rice husk ash as a bio-filler for application in direct methanol fuel cells. *Int J Hydrogen Energy* 2019;44:1857–1866.
- [25] Ranjani M., Pannipara M., Al-Sehemi A.G., Vignesh A. Chitosan/sulfonated graphene oxide/silica nanocomposite membranes for direct methanol fuel cells. *Solid State Ionics* 2019;338:153–160.
- [26] Mokrini A., del Río C., Acosta J.L. Synthesis and characterization of new ion conductors base on butadiene styrene copolymers. *Solid State Ionics* 2004;166:375–381.
- [27] Navarro A., del Río C., Acosta J.L. Kinetic study of the sulfonation of hydrogenated styrene butadiene block copolymer (HSBS). Microstructural and electrical characterization. *J Membr Sci* 2007;300:79–87.
- [28] del Rio C., García O., Morales E., Escribano P.G. Single cell performance and electrochemical characterization of photocrosslinked and post-sulfonated SEBS-DVB membranes. *Electrochim Acta* 2015;176:378–387.
- [29] Orujalipoor I., Polat K., Huang Y.C., İde S., ŞenM, Jeng U.S., et al. Partially sulfonated styrene-(ethylene-butylene)-styrene copolymers: nanostructures, bio and electro-active properties. *Mater Chem Phys* 2019;225:399–405.
- [30] Jung D.H., Myoung Y.B., Cho S.Y., Shin D.R., Peck D.H. A performance evaluation of direct methanol fuel cell using impregnated tetraethyl-orthosilicate in cross-linked polymer membrane. *Int J Hydrogen Energy* 2001;26:1263–1269.
- [31] Liu K.L., Lee H.C., Wang B.Y., Lue S.J., Lu C.Y., Tsai L.D., et al. Sulfonated poly(styrene-block-(ethylene-ran-butylene)-block-styrene (SSEBS)-zirconium phosphate (ZrP) composite membranes for direct methanol fuel cells. *J Membr Sci* 2015;495:110–120.
- [32] Wang B.Y., Tseng C.K., Shih C.M., Pai Y.L., Kuo H.P., Lue S.J. Polytetrafluoroethylene (PTFE)/silane cross-linked sulfonated poly(styrene-ethylene/butylene-styrene) (sSEBS) composite membrane for direct alcohol and formic acid fuel cells. *J Membr Sci* 2014;464:43–54.
- [33] Hwang H.Y., Kim S.J., Oh D.Y., Hong Y.T., Nam S.Y. Proton conduction and methanol transport through sulfonated poly(styrene-b-ethylene/butylene-b-styrene)/clay nanocomposite. *Macromol Res* 2011;19:84–89.

- [34] Choa H.D., Wona J., Ha H.Y. Composite polymer electrolyte membranes containing polyrotaxanes. *Renew Energy* 2008;33:248–253.
- [35] Won J., Cho H.D. The effect of annealing on sSEBS/polyrotaxanes electrolyte membranes for direct methanol fuel cells. *Macromol Res* 2009;17:729–733.
- [36] Mistry M.K., Choudhury N.R., Dutta N.K., Knott R. Inorganic modification of block copolymer for medium temperature proton exchange membrane application. *J Membr Sci* 2010;351:168–177.
- [37] Heo P., Shen Y., Kojima K., Pak C., Choi K.H., Hibino T. $\text{Fe}_{0.4}\text{Ta}_{0.5}\text{P}_2\text{O}_7$ -based composite membrane for high-temperature, low-humidity proton exchange membrane fuel cells. *Electrochim Acta* 2014;128:287–291.
- [38] Jin Y., Fujiwara K., Hibino T. High temperature, low humidity proton exchange membrane based on an inorganic–organic hybrid structure. *Electrochem Solid State Lett* 2010;13:B8–B10.
- [39] Lue S.J., Liu N.Y., Kumar S.R., Tseng K.C.Y., Wang B.Y., Leung C.H. Experimental and one-dimensional mathematical modeling of different operating parameters in direct formic acid fuel cells. *Energies* 2017;10:1972–1986.
- [40] Sivasankaran A., Sangeetha D., Ahn Y.H. Nanocomposite membranes based on sulfonated polystyrene ethylene butylene polystyrene (SSEBS) and sulfonated SiO_2 for microbial fuel cell application. *Chem Eng J* 2016;289:442–451.
- [41] Rezakazemi M., Sadrzadeh M., Mohammadi T., Matsuura T. Methods for the preparation of organic-inorganic nanocomposite polymer electrolyte membranes for fuel cells. In: Inamuddin MA, Asiri AM, editors. *Organic-inorganic composite polymer electrolyte membranes: preparation, properties, and fuel cell applications*. Springer International Publishing; 2017. p. 311–325.
- [42] Pourzare K., Mansourpanah Y., Farhadi S. Advanced nanocomposite membranes for fuel cell applications: a comprehensive review. *Biofuel Res J* 2016;12:496–513.
- [43] Kim D.J., Jo M.J., Nam S.Y. A review of polymer–nanocomposite electrolyte membranes for fuel cell application. *J Ind Eng Chem* 2015;21:36–52.
- [44] Mishra A.K., Bose S., Kuila T., Kim N.H., Lee J.H. Silicate-based polymer-nanocomposite membranes for polymer electrolyte membrane fuel cells. *Prog Polym Sci* 2012;37:842–869.
- [45] Mosa J., Aparicio M. Sol-gel materials for batteries and fuel cells. In: Levy D, Zayat M, editors. *The sol-gel handbook: synthesis, characterization and applications*. Wiley-VCH Verlag GmbH & Co. KGaA; 2015. p. 1071–1117.
- [46] Tripathi B.P., Shahi V.K. Organic–inorganic nanocomposite polymer electrolyte membranes for fuel cell applications. *Prog Polym Sci* 2011;36:945–979.

- [47] Li S., Liu M. Synthesis and conductivity of proton-electrolyte membranes based on hybrid inorganic–organic copolymers. *Electrochim Acta* 2003;48:4271–4276.
- [48] Gómez-Romero P., Asensio J.A., Borrós S. Hybrid proton-conducting membranes for polymer electrolyte fuel cells: phosphomolybdic acid doped poly (2, 5-benzimidazole)—(ABPBI-H3PMo12O40). *Electrochim Acta* 2005;50:4715–4720.
- [49] Mauritz K.A., Mountz D.A., Reuschle D.A., Blackwell R.I. Self-assembled organic/inorganic hybrids as membrane materials. *Electrochim Acta* 2004;50:565–569.
- [50] Kwee T., Taylor S.J., Mauritz K.A., Storey R.F. Morphology and mechanical and dynamic mechanical properties of linear and star poly(styrene-b-isobutylene-b-styrene) block copolymers. *Polymer* 2005;46:4480–4491.
- [51] Blackwell R.I., Mauritz K.A. Nanostructured organic/inorganic materials based on sol/gel processes in sulfonated poly(styrene-co-(ethylene-butylene)-co-styrene (SEBS) block copolymers. *Am Chem Soc, Div Polym Chem* 2002;43:1341–1342.
- [52] Mauritz K.A., Storey R.F., Mountz D.A., Reuschle D.A. Poly(styrene-b-isobutylene-b-styrene) block copolymer ionomers (BCPI), and BCPI/silicate nanocomposites. 1. Organic counterion: BCPI sol–gel reaction template. *Polymer* 2002;43:4315–4323.
- [53] Chen H., Hassan M.K., Peddini S.K., Mauritz K.A. Macromolecular dynamics of sulfonated poly(styrene-b-ethylene-ran-butylene-b-styrene) block copolymers by broadband dielectric spectroscopy. *Eur Polym J* 2011;47:1936–1948.
- [54] Peddini S.K., Pham H.N., Spinu L., Weston J.L., Nikles D.E., Mauritz K.A. Morphology and magnetic properties of sulfonated poly[styrene–(ethylene/butylene)–styrene]/iron oxide composites. *Eur Polym J* 2015;69:85–95.
- [55] Mosa J., Larramona G., Durán A., Aparicio M. Synthesis and characterization of P2O5–ZrO2–SiO2 membranes doped with tungstophosphoric acid (PWA) for applications in PEMFC. *J Membr Sci* 2008;307:21–27.
- [56] Mosa J., Aparicio M., Durán A., Castro Y. Mesostructured HSO3-functionalized TiO2–P2O5 sol-gel films prepared by evaporation induced self-assembly method with high proton conductivity. *Electrochim Acta* 2015;173:215–222.
- [57] Castro Y., Mosa J., Aparicio M., Pérez-Carrillo L.A., Vílchez S., Esquena J., et al. Sol–gel hybrid membranes loaded with meso/macroporous SiO2, TiO2–P2O5 and SiO2–TiO2–P2O5 materials with high proton conductivity. *Mater Chem Phys* 2015;149:686–694.
- [58] Castro Y., Mosa J., Durán A. Recubrimientos meso-porosos de SiO2-TiO2-P2O5 para aplicaciones en pilas de combustible de intercambio protónico. *Bol Soc Espanola Ceram Vidr* 2014;53:171–178.

- [59] Mosa J., Durán A., Aparicio M. Sulfonic acid-functionalized hybrid organic-inorganic proton exchange membranes synthesized by sol-gel using 3-mercaptopropyl trimethoxysilane (MPTMS). *J Power Sources* 2015;297:208–216.
- [60] Escribano P.G., del Río C., Morales E., Aparicio M., Mosa J. Infiltration of 40SiO₂–40P₂O₅–20ZrO₂ sol-gel in sSEBS membranes for PEMFCs application. *J Membr Sci* 2018;551:136–144.
- [61] Jurado J.R., Chinarro E., Colomer M.T. Pat No. ES 2 209 657. 2005.
- [62] Ren X., Springer T.E., Zawodzinski T.A., Gottesfeld S. Methanol transport through nation membranes. Electro-osmotic drag effects on potential step measurements. *J Electrochem Soc* 2000;147:466–474.
- [63] Leo T.J., Raso M.A., Navarro E., de la Blanca E.S., Villanueva M., Moreno B. Response of a direct methanol fuel cell to fuel change. *Int J Hydrogen Energy* 2010;35:11642–11648.
- [64] Yang J.E., Lee J.S. Selective modification of block copolymers as proton exchange membranes. *Electrochim Acta* 2004;50:617–620.
- [65] Rodriguez J.I.C., Ladewig B.P., Dicks A.L., Duke M.C., Martin D.J., Lu G., et al. Nanocomposite Nafion-silica membranes for direct methanol fuel cells. *World hydrogen technology conference*; 2005. p. 1–8.
- [66] Ranjani M., Yoo D.J., Kumar G.G. Sulfonated Fe₃O₄@ SiO₂ nanorods incorporated sPVdF nanocomposite membranes for DMFC applications. *J Membr Sci* 2018;555:497–506.
- [67] Miyake N., Wainright J.S., Savinell R.F. Evaluation of a sol-gel derived Nafion/silica hybrid membrane for polymer electrolyte membrane fuel cell applications: II. Methanol uptake and methanol permeability. *J Electrochem Soc* 2001;148:A905–A909.
- [68] del Río C., Jurado J.R., Acosta J.L. Hybrid membranes based on block co-polymer ionomers and silica gel. Synthesis and characterization. *Polymer* 2005;46:3975–3985.
- [69] Kumar G.G., Manthiram A. Sulfonated polyether ether ketone/strontium zirconite@ TiO₂ nanocomposite membranes for direct methanol fuel cells. *J Mater Chem A* 2017;5:20497–20504.
- [70] Kumar G.G., Shin J., Nho Y.C., Hwang I.S., Fei G., Kim A.R., et al. Irradiated PVdF-HFP–tin oxide composite membranes for the applications of direct methanol fuel cells. *J Membr Sci* 2010;350:92–100.
-

Highlights

- Zirconia phosphosilicate-sSEBS membranes are prepared by sol-gel infiltration.
 - Incorporation of inorganic phase into hydrophilic domains is confirmed by AFM and DMA.
 - Infiltration induces strong hydrogen bond interactions between Si–OH, P–OH and SO₃H.
 - Methanol crossover decreases over infiltration time and is lower than sSEBS and N112.
 - Best DMFC performance is reported for the hybrid membrane infiltrated for 40 min.
-

Queries and Answers

Query: Your article is registered as belonging to the Special Issue/Collection entitled “HYCELTEC 2019 (Piscina”. If this is NOT correct and your article is a regular item or belongs to a different Special Issue please contact d.norman@elsevier.com immediately prior to returning your corrections.

Answer: Yes

Query: Please confirm that given names and surnames have been identified correctly and are presented in the desired order and please carefully verify the spelling of all authors' names.

Answer: Yes

Query: Please note that author’s telephone/fax numbers are not published in Journal articles due to the fact that articles are available online and in print for many years, whereas telephone/fax numbers are changeable and therefore not reliable in the long term.

Answer: Thank you for the information. The data provided are correct.

Query: Please confirm that the provided email “oscar.santiago.carretero@upm.es” is the correct address for official communication, else provide an alternate e-mail address to replace the existing one, because private e-mail addresses should not be used in articles as the address for communication.

Answer: The email provided is correct.

Query: Have we correctly interpreted the following funding source(s) and country names you cited in your article: Comunidad de Madrid, Spain; European Social Fund (ESF), European Union?

Answer: Yes

